doi: 10.15407/ujpe62.05.0432

V.O. YUKHYMCHUK,[1] M.YA. VALAKH,[1] O.M. HRESHCHUK,[1] YE.O. HAVRYLYUK,[1] I.B. YANCHUK,[1] A.V. YEFANOV,[1,2] R.N. ARIF,[3] A.G. ROZHIN,[3] M.A. SKORYK[2]

[1] V.E. Lashkaryov Institute of Semiconductor Physics, Nat. Acad. of Sci. of Ukraine
(41, Prosp. Nauky, Kyiv 03028, Ukraine; e-mail: hreshchuk@gmail.com)
[2] Nanomedtech LLC
(68, Antonovych Str., Kyiv 03680, Ukraine)
[3] Electronic Engineering Division, School of Engineering & Applied Science
(Aston University, Aston Triangle, Birmingham, B4 7ET, UK)

PROPERTIES OF GRAPHENE FLAKES OBTAINED BY TREATING GRAPHITE WITH ULTRASOUND

PACS 33.20.Fb, 61.48.Gh, 78.67.Wj

A possibility to obtain graphene and graphene layers with the help of the ultrasound (US) treatment of pyrolytic graphite in an N-methyl pyrrolidone (NMP) solution has been demonstrated. Raman spectroscopy is confirmed to be an effective method for monitoring the graphite transformation into graphene. By varying the time of the ultrasonic treatment of pyrolytic graphite in the NMP solution, optimum regimes for the fabrication of graphene flakes with various numbers of layers are determined. In particular, the US treatment for 5 h is shown to be sufficient for producing a colloidal solution of graphene flakes, most of which are single-layered. It is shown that the longer US treatment results in larger intensities of Raman bands D and D′, which testifies to a larger number of defects in the graphene layers. The average distances between defects are estimated for various times of US treatment. The influence of vacancy and edge defects on the intensity band ratio $I_D/I_{D'}$ is analyzed. Vacancies are found to be the prevailing type of defects in the graphene flakes.

K e y w o r d s: graphene, Raman spectroscopy, ultrasound treatment, vacancy and edge defects, scanning electron microscopy.

1. Introduction

Nowadays, graphene is one of the most promising materials for modern nanoelectronics [1–4]. Its fundamental properties differ drastically from the properties of 3D materials and find their manifestation in the extreme graphene parameters. In particular, we should mark an almost ballistic transport of charge carriers at room temperature, the electric and thermal conductivities that are the highest among all substances, the highest strength among crystalline materials, chemical stability, and so forth. The high transparency of graphene allows it to be also used in optoelectronics.

After graphene was obtained in 2004 [5] by mechanically exfoliating separate layers from graphite, a boom in the research of its properties arose. Numerous researches have already demonstrated the future advantage of the use of graphene for solar cells [6], supercapacitors [7], optoelectronic devices [8], biosensors [9], SERS substrates [10], catalysts [11], nanofluids [12], high-frequency transistors [13], *etc.* The graphene properties can be substantially different depending on the method of fabrication, because the size of graphene flakes, the number of defects in them (in particular, vacancy or edge ones) change at that. Moreover, the graphene properties are considerably affected by the parameters of a substrate, onto which graphene has been deposited [14].

Note that the research of graphene properties and the manufacture of devices on its basis are not restricted to single-layered specimens. Structures with two and more layers (up to 10) are also of interest. Therefore, new data about graphene and ultrathin graphene films are important for the creation of

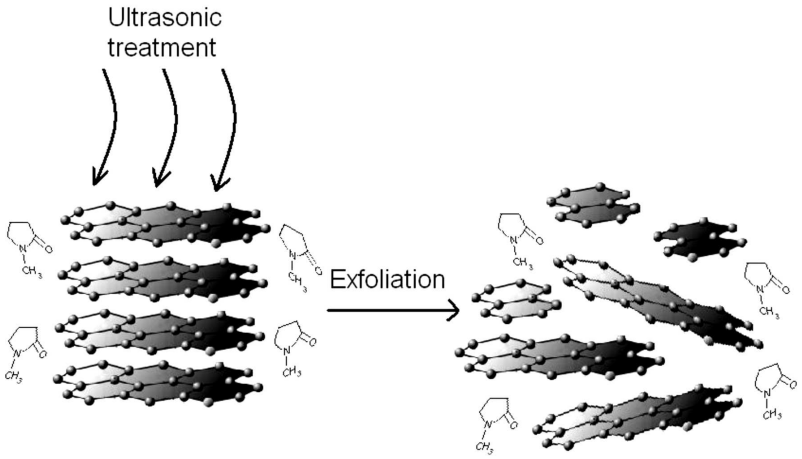

Fig. 1. Schematic diagram of the fabrication of graphene flakes with the help of the ultrasound treatment of graphite in the NMP solution

a general physical picture of its properties and for the development of devices for nano- and optoelectronics. Now, the main methods of graphene fabrication are the graphite intercalation [5], chemical vapor deposition (CVD) epitaxy [15], high-temperature graphitization of SiC [16], high-temperature sublimation of polycrystalline SiC [17], and others. Each of the mentioned methods has its advantages and shortcomings. In particular, graphene flakes obtained by the intercalation have different sizes, the method of CVD epitaxy is rather expensive, and the graphitization of SiC does not allow the obtained layers to be transferred onto other substrates.

All the aforesaid stimulates a permanent search for efficient methods of production of graphene and ultrathin films on its basis. In work [18], a method of graphene manufacture by centrifugating the graphite solution in N-methyl-2-pyrrolidone (NMP) or in an aqueous solution with the NaC surfactant was demonstrated. Today, this is the most productive way of graphene production.

In this work, we consider a method of graphene fabrication, which combines two factors: the weakening of the interaction between graphite layers by introducing molecules of various substances therein, and the following action of ultrasound with a certain frequency and energy on graphite (Fig. 1). The ultimate exfoliation of graphene flakes from graphite nanocrystallites was performed with the help of the centrifugation. The work is aimed at the development of an efficient method for producing the graphene flakes and at the research of their properties. Raman

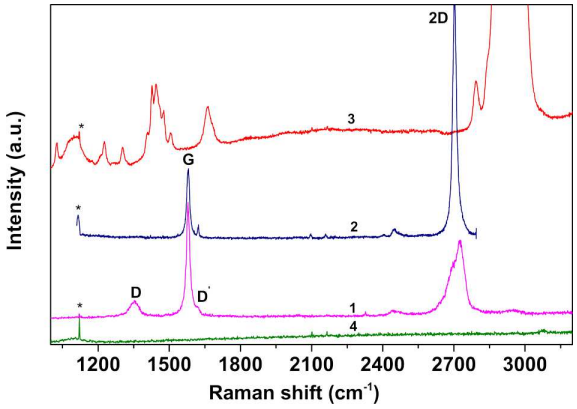

Fig. 2. Raman spectra of graphite (*1*), graphene (*2*), SDBS (*3*), and NMP (*4*). Bands induced by radiation of the discharge plasma in an Ar^+-laser are marked by asterisks

spectroscopy is applied as a basic research method. It is non-destructive, fast, and sensitive to disordering effects in sp^2 carbon structures.

2. Experimental Technique

Highly oriented pyrolitic graphite was used as an initial material for the graphene production. Graphite was put into an US bath with various solutions: N-methyl pyrrolidone (NMP) and sodium dodecyl benzene sulfonate (SDBS). The vibrational modes of organic solvents may manifest themselves in the Raman spectra in the spectral region that are typical of just graphite and graphene films (Fig. 2, curves *1* and *2*). Therefore, it is important to verify that the sol-

vent used for weakening bonds between graphite layers induces no such bands in the Raman spectrum.

In the Raman spectrum of SDBS (Fig. 2, curve *3*), a number of high-intensity bands are observed near the graphene ones. Our researches showed that the presence of SDBS molecules on graphene layers does not allow the frequency position and the intensity of graphene bands to be determined properly, which is important for their correct interpretation. At the same time, the aqueous solution of N-methyl pyrrolidone has only low-intensive bands with maxima at 1100 and 3080 cm^{-1} in this spectral interval. That is why the NMP solution was used further for elaborating the technology of graphene fabrication.

In order to prepare the working solution, 5 mg of graphite were dissolved in 20 ml of NMP. Afterward, the solution was treated with ultrasound with a frequency of 21 kHz and a power of 250 W. The time of the US treatment of graphite was varied from 30 min to 5 h. To avoid the degradation of a solution owing to its heating under the US action, the treatment was interrupted every 30 min. The interaction between molecules of the NMP solution and graphite is known to result in a weakening of the interaction between separate graphite layers, whereas US makes it possible to exfoliate separate graphene layers with various thicknesses from graphite clusters. As a result of this US treatment, a colloidal solution was formed from carbon nanoparticles with different masses. Their mass separation was carried out on a centrifuge during 30 min at a rotational velocity of about 8×10^3 min^{-1}. The solutions of carbon nanostructures obtained in such a way were deposited onto glass substrates and heated during several seconds to 80 °C in air.

The obtained carbon films were studied using the Raman spectroscopy on an installation Ranishaw-1000. The spectra were excited with the help of radiation emitted by an Ar^+-laser with a wavelength of 514.5 nm and focused on graphene structures be means of an 50x objective. For Raman studies, the concentration of graphene flakes in the solution was selected rather low, which allowed us to obtain graphene flakes on the glass surface without their mutual superposition.

3. Results and Their Discussion

In Fig. 3, SEM images of micron-sized graphite particles before their treatment (*a*) and after the 60-min US treatments in the NMP solution (*b* and *c*) are exhibited. The last two images allow us to draw a conclusion that, after the ultrasound treatment, the solution contains both micron-sized graphite crystallites and graphene flakes. In Fig. 3, *c*, one can observe graphene flakes on the surface of a graphite crystallite; in particular, a light rectangle is used to distinguish an almost rectangular graphene flake. Figure 3, *d* demonstrates an SEM image of graphene flakes after their separation on a centrifuge. The concentration of flakes in the solution for SEM researches was rather high, so that they overlapped one another on the glass surface. It is rather difficult to evaluate the number of layers in graphene flakes by means of SEM. Therefore, Raman spectroscopy was used for their quantitative characterization.

As was indicated above, solutions with insignificant concentrations of graphene flakes were used for Raman researches. In Fig. 4, Raman spectra of an initial graphite film (*1*) and graphene films with various numbers of layers (*2* to *5*) obtained by the US treatment with the following separation on a centrifuge are shown. The power and frequency of the US treatment of specimens were identical in all cases, and the treatment time was varied from 0.5 to 5 h.

In order to make the further analysis convenient, all spectra were normalized to the G band intensity. From the figure, one can see how the Raman spectra change in time, when graphite (curve *1*) transforms into graphene flakes (curves *2* to *5*) under the US treatment in the NMP solution. Note that, after each 1-h interval of the US treatment, a large number of spectra were measured for various graphene flakes (Fig. 5). As one can see from the figure, most of the spectra are rather similar to one another with identical ratios between the band intensities. However, there are spectra that differ a little from the others (see spectrum *4* with the enhanced intensity of the D band). Figure 4 illustrates the most typical spectra for the majority of graphene flakes obtained after each treatment stage.

It is known that, for graphene and graphite, the Raman spectrum of the first order always contains the so-called G band (at 1582 cm^{-1}). It is related to the doubly degenerate symmetry mode E_{2g} of the Brillouin zone center and is a manifestation of stretching vibrations of all pairs of carbon atoms that are sp^2-hybridized and are located in benzene rings [19,20]. If

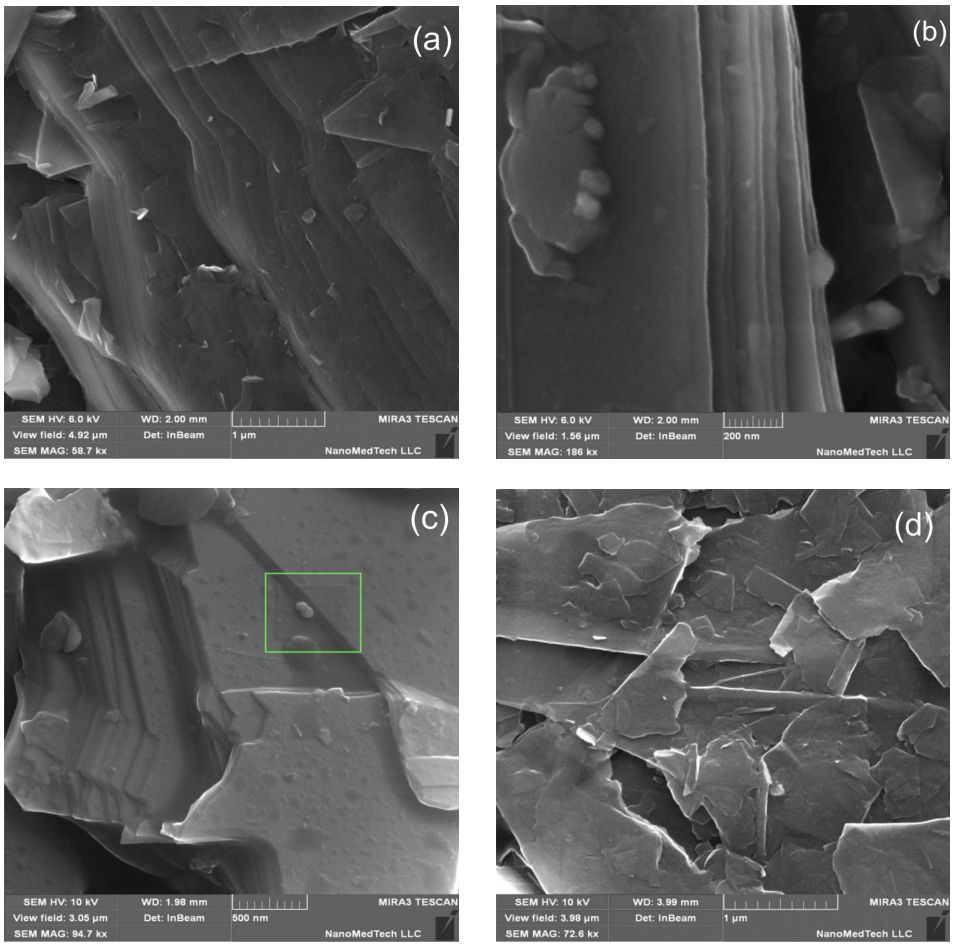

Fig. 3. SEM images of graphite areas before (*a*) and after the 60-min US treatment without centrifugation (*b* and *c*). A light rectangle marks one of the graphene flakes on the graphite surface. (*d*) Graphene flakes after deposition on a glass substrate from the solution subjected to the centrifugation and, sequentially, US treatment for 60 min (*d*)

carbon structures contain defects, their spectra reveal the so-called D (at 1350 cm^{-1}) and D' (at 1620 cm^{-1}) bands. The D band is a manifestation of A_{1g} breathing modes at point K at the boundary of the Brillouin zone of sp^2-hybridized carbon atoms in the benzene rings. It is registered in Raman spectra only for specimens with defects, being forbidden by selection rules in defect-free structures [19, 20]. It is known that if the size of carbon crystallites diminishes, the intensity ratio for the D and G bands grows [21]. This is a consequence of the fact that a reduction of crystallite dimensions increases the number of surface defects, whereas the number of modes connected with stretching vibrations (they give a contribution to the G band) decreases, because the total number of atoms in crystallites becomes smaller.

We would like to attract attention to some other features in those bands, because their knowledge is important both when the Raman spectra of carbon structures are measured and when they are interpreted. The D band is characterized by a strong dispersion dependence on the exciting radiation energy (about 50 $\mathrm{cm}^{-1}/\mathrm{eV}$). This dependence is a result of the so-called Kohn anomaly located near point K in the Brillouin zone [22]. Therefore, if the energy of exciting laser radiation increases, the D band shifts to the high-frequency region, and its intensity decreases. This fact is important to be taken into con-

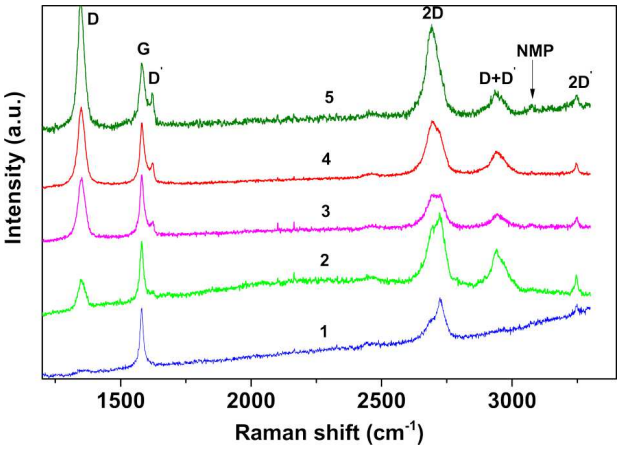

Fig. 4. Raman spectra of initial pyrolytic graphite (*1*) and graphene layers obtained after various times of the US treatment in the NMP solution: 30 (*2*), 60 (*3*), 120 (*4*), and 300 min (*5*). The spectra are normalized to the G band intensity

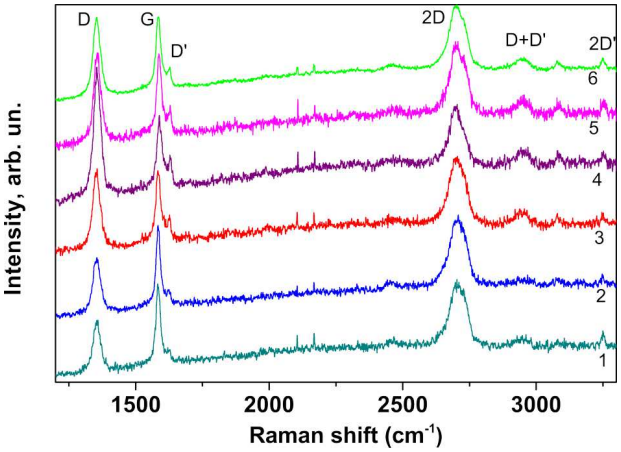

Fig. 5. Raman spectra of five different graphene flakes obtained after the 60-min US treatment (*1–5*) and the averaged spectrum (*6*). The spectra are normalized to the G band intensity

sideration, when choosing laser radiation for the excitation and when analyzing the I_D/I_G ratio. As was marked above, for the D' band (1620 cm^{-1}) to manifest itself in Raman spectra, the presence of defects is also required. This requirement is related to the necessity to obey the momentum conservation law for phonons. At the same time, vibrations that are responsible for the D' band have certain distinctions from vibrations in the D mode, which will be discussed below.

A specific feature of Raman spectra for graphene in comparison with those for graphite is that the intensity of the $2D$ band is higher than the intensity of the G band, and, if the number of graphene layers increases, the ratio I_{2D}/I_G decreases [20, 23]. This feature is a result of the fact that only graphene is characterized by a large cross-section of Raman scattering due to the double resonance of exciting and scattered radiation with optical transitions in its electron structure. However, if the number of defects in graphene increases, the ratio I_{2D}/I_G decreases [24].

Note that the number of graphene layers also substantially affects the shape and the frequency position of the $2D$ band [20, 24]. Single-layered graphene is characterized by the intense symmetric $2D$ band (Fig. 2, curve *2*). If the number of graphene layers increases to two, the $2D$ band becomes a superposition of four bands with different intensities [20, 24], as was observed in our spectra as well (Fig. 4, curve *4*).

Note also that the ratio I_{2D}/I_G strongly depends on the energy of exciting laser radiation and the graphene doping. In the latter case, if the doping is low, the position of the G band equals about 1580 cm^{-1} [25], and the $2D$ band is 2 to 5 times more intense than the G band, depending on exciting radiation. At a high doping level, the G band is located at about 1600 cm^{-1}, and $I_{2D}/I_G \sim 1$ [25].

Let us analyze our experimental Raman spectra exhibited in Fig. 4. As was indicated above, for the more convenient interpretation, all spectra were normalized to the G band intensity. Its frequency position (at 1581–1582 cm^{-1}) for initial graphite and graphene flakes testifies that the specimens are undoped [25]. Curve *1* corresponds to initial pyrolytic graphite. In this spectrum, the D band has a low intensity, and the D' band does not manifest itself at all, which testifies that initial graphite contains few defects. From Fig. 4, one can see that, as the time of the treatment by US increases, the relative intensity of the D and D' bands also grows. This behavior may testify that either the average size of carbon films decreases [21] or the number of non-edge defects in the graphene films grows [26, 27].

In order to determine the parameters of separate bands, the experimental spectra were resolved into Lorentzian components, as is shown in Fig. 6 for specimen No. 5. Using the formula [28]

$$L_D(\text{nm}) = 560E_l^4(I_D/I_G)^{-1}, \qquad (1)$$

Parameters of the bands

No.	t, min	ν_D, cm^{-1}	I_D	Γ_D, cm^{-1}	ν_G, cm^{-1}	I_G	Γ_G, cm^{-1}	I_D/I_G	$I_D/I_{D'}$	L_D, nm	D, cm^{-1}
1	0	1355	2399.1	30.0	1581	18714.7	15.7	0.13	–	130.0	–
2	30	1350	14810.4	31.1	1581	14618.4	16.2	1.01	7.1	16.4	1621.1
3	60	1350	41589.7	31.9	1582	23169.6	18.9	1.80	7.6	9.2	1619.5
4	120	1350	92008.8	30.7	1582	47380.8	21.3	1.94	8.6	8.6	1620.5
5	300	1347	95004	29.0	1582	41425	27.3	2.29	10.09	7.2	1621.9

we evaluated the average distance between the defects in graphene flakes. In formula (1), the energy of exciting laser radiation E_l is reckoned in electronvolt units (eV). The obtained L_D values are quoted in Table.

The analysis of Raman spectra *2* to *5* in Fig. 4 and the parameters of their bands (Table) testifies that the graphene flakes had from 1 to 4 layers. Really, as is seen from the spectra, the intensity of $2D$ bands is comparable or higher than that of G bands. However, one can also see that those bands in spectra *2* to *4* consist of a few components. The resolution of those bands into separate components testifies that spectrum *2* corresponds to four-layer, spectrum *3* to three-layer, and spectrum *4* to two-layer graphene.

Spectrum 5 corresponds to one-layer graphene. Really, the $2D$ band has a symmetric shape, a considerable intensity ($I_{2D}/I_G = 1.45$), and a frequency of 2694 cm^{-1}. It should be noted that even after the 30-min US treatment, the solution contained one-layer graphene flakes; however, the figure exhibits only the spectra that correspond to the majority of available flakes. From the spectra, one can see that all $2D$ bands have a larger halfwidth; in particular, for monolayer graphene, this parameter equals 58 cm^{-1}. This is a result of a significant number of defects inserted into graphene layers during the US treatment and the centrifugation. Bands with similar parameters were observed in works [14, 18], and the corresponding band shapes and halfwidths correlate well with the parameters of our bands.

In order to estimate which defects dominate in the graphene flakes produced by the proposed method, we have analyzed the obtained Raman spectra. It is clear that the increase of the time of the treatment by US results not only in a better exfoliation of graphene flakes from graphite crystals, but also in a reduction of flake dimensions. The number of edge defects grows at that. On the other hand, as one can see from Table, a longer US treatment decreases the average distance between defects from 16.4 nm at 30 min to 7.2 nm at 5 h, which testifies to the growth in the number of vacancy and other structural defects.

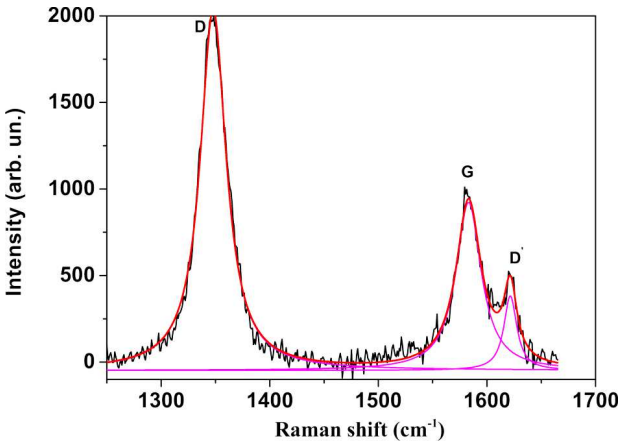

Fig. 6. Raman spectrum of carbon film No. 5 in the spectral interval of the D and G bands, and its resolution into separate components

As is seen from Fig. 4 (curve *1*), the Raman spectrum of initial graphite contains the low-intensity D band located at a frequency of 1350 cm^{-1} and associated with the presence of defects. However, this fact does not mean that the nanolayers exfoliated from graphite also contain defects in their planes. The edges of those nanolayers can manifest themselves as defects that make or do not make contribution to the D band, because the result depends on the edge quality [23]. In particular, it was shown in work [29] that the "armchair" graphite edge gives a substantial contribution to the D band, unlike the "zigzag" edge, which is associated with different directions of the wave vectors of defects connected with those edges. At the same time, the defects of both edge types contribute to the D' band intensity. It is so because the process of D' mode activation occurs in one valley of the Brillouin zone near point K or K'. This

is in contrast to the D mode, which allows defect's wave vector to connect any two points at the circle on the cone-like energy surface in the Brillouin zone [30].

Another basic difference between the D and D' modes manifests itself, if the defect concentration in graphite or graphene is high. If the average distance between defects diminishes to 5 nm or less, the D band intensity starts to drastically decrease [24, 26], because the number of defect-free benzene rings that take part in the Raman scattering diminishes. At the same time, the D' band intensity continues to grow under those conditions. Such distinctions in the behaviors of those two modes allow them to be used not only for the quantitative characterization of available defects, but also for the establishment of their dominating type.

This possibility was demonstrated in work [31], where it was shown that the intensity ratio for the D and D' bands can be used to characterize defects in graphene layers with moderate imperfection. If the number of defects is significant, the ratio $I_D/I_{D'}$ can be used until the G and D' bands do not overlap, and the the intensity of the latter can be determined accurately. Really, as was shown in works [24, 31], the dependences of the intensities of those bands on the number of defects are different. In work [31], it was pointed out that $I_D = A \times n$ and $I_{D'} = B \times n$, where n is the number of defects, and A and B are proportionality coefficients with different values, which is associated with different origins of those defects.

In works [18, 31], it was shown that the value of ratio $I_D/I_{D'}$ between the intensities of Raman bands for graphene flakes, when falling within an interval from 3 to 4.5, means that the flakes contain only edge defects. The $I_D/I_{D'}$ values from 4.5 to 7.5 determine the limits typical of graphene flakes with vacancy and edge defects. The ratios from about 7.5 to about 13 characterize graphene, in which defects of the vacancy type dominate. As one can see from Table, the values of ratio $I_D/I_{D'}$ for the carbon nanostructures analyzed by us vary from 7 to 10. It is clear that graphene flakes have edge defects in any case. However, on the basis of the values of $I_D/I_{D'}$, we may assert that defects of the vacancy type prevail in the graphene flakes in our case.

In work [32], it was demonstrated that the point-like and linear defects of various types can substantially change the physical, magnetic, and chemical properties of graphene. The analysis of the number of defects and their type is also important, when graphene is used in nanocatalysis. This statement is confirmed by a growing number of works devoted exactly to this scope of applications of graphene [33].

4. Conclusions

To summarize, a possibility to enhance the efficiency of the fabrication of graphene and graphene-based layers by applying the US treatment to the solution of pyrolytic graphite in N-methyl pyrrolidone (NMP) is demonstrated. Raman spectroscopy is confirmed to be an efficient method for the diagnostics of the transformation of graphite into graphene. The variation of the time of the ultrasonic treatment of pyrolytic graphite in an NMP solution allowed us to determine the optimum regimes for the production of graphene flakes with various numbers of layers. In particular, the US treatment of graphite for 5 h with following centrifugation is shown to be enough for the manufacture of a colloidal solution of graphene flakes, the majority of which are single-layered. It is shown that the longer times of the US treatment increase the intensity of Raman bands D and D', which testifies to a growth of the number of defects in graphene layers. The average distances between the defects are estimated for various times of the US treatment. They are found to vary from 16.4 nm at the 30-min treatment to 7.2 nm at the 5-h one. The influence of vacancy and edge defects on the ratio $I_D/I_{D'}$ is analyzed. It is found that the vacancy defects prevail in the produced graphene flakes. Since the defects of different types in graphene can stimulate different changes of its physico-chemical properties, the determination of the defect type could be useful in the future, while tuning the graphene parameters in accordance with the requirements of a specific task.

This work was executed in the framework of the Marie Curie International Research Staff Exchange Scheme "TelaSens" project, Research Executive Agency Grant No. 269271, Programme: FP7-PEOPLE-2010-IRSES.

1. K.S. Novoselov, V.I. Fal'ko, L. Colombo, P.R. Gellert, M.G. Schwab, K. Kim. A roadmap for graphene. *Nature* **490**, 192 (2012).
2. X. Yang, C. Cheng, D. Sichao, Y. Jianyi, Y. Bin, L. Jack, Y. Wenyan, L. Erping, D. Shurong, Y. Peide, D. Xiangfeng. Contacts between two- and three-dimensional materials:

Ohmic,Schottky, and *p-n* heterojunctions. *ACS Nano* **10**, 4895 (2016).
3. S. Chen, S. Zhimei, L. Feng. Strain engineering of graphene: A review. *Nanoscale* **8**, 3207 (2016).
4. A.N. Morozovska, E.A. Eliseev, M.V. Strikha. Ballistic conductivity of graphene channel with *p-n* junction on ferroelectric domain wall. *Appl. Phys. Lett.* **108**, 232902 (2016).
5. K.S. Novoselov, A.K. Geim, S.V. Morozov, D. Jiang, Y. Zhang, S.V. Dubonos, I.V. Grigorieva, A.A. Firsov. Electric field effect in atomically thin carbon films. *Science* **306**, 666 (2004).
6. A.A. Tahir, H. Ullah, P. Sudhagar, M.A.M. Teridi, A. Devadoss, S. Sundaram. The application of graphene and its derivatives to energy conversion, storage, and environmental and biosensing devices. *Chem. Rec.* **16**, 1591 (2016).
7. Wen Yang, Mei Ni, Xin Ren, Yafen Tian, Ning Li, Yuefeng Su, Xiaoling Zhang. Graphene in supercapacitor applications. *Curr. Opin. Coll. Interface Sci.* **20**, 416 (2015).
8. A. Bablich, S. Kataria, M.C. Lemme. Graphene and two-dimensional materials for optoelectronic applications. *Electronics* **5**, 13 (2016).
9. Z. Chengzhou, D. Dan, L. Yuehe. Graphene-like 2D nanomaterial-based biointerfaces for biosensing applications. *Biosens. Bioelectron.* **89**, 43 (2017).
10. K. Leilei, C. Jiayu, Z. Hongtao, X. Ping, S. Mengtao. Recent progress in the applications of graphene in surface-enhanced Raman scattering and plasmon-induced catalytic reactions. *Mater. Chem. C* **3**, 9024 (2015).
11. B.F. Machado, P. Serp. Graphene-based materials for catalysis. *Catalys. Sci. Technol.* **2**, 54 (2012).
12. E. Sadeghinezhad, M. Mehrali, R. Saidur, M. Mehrali, S.T. Latibari, A.R. Akhiani, H.S.C. Metselaar. A comprehensive review on graphene nanofluids: recent research, development and applications. *Ener. Conv. Manag.* **111**, 466 (2016).
13. F. Schwierz. Graphene transistors. *Nature Nanotech.* **5**, 487 (2010).
14. A. Das, B. Chakraborty, A.K. Sood. Raman spectroscopy of graphene on different substrates and influence of defects. *Bull. Mater. Sci.* **31**, 579 (2008).
15. A. Guermoune, T. Chari, F. Popescu, S.S. Sabri, J. Guillemette, H.S. Skulason, T. Szkopek, M. Siaj. Chemical vapor deposition synthesis of graphene on copper with methanol, ethanol, and propanol precursors. *Carbon* **49**, 4204 (2011).
16. N. Camara, J.-R. Huntzinger, G. Rius, A. Tiberj, N. Mestres, F. Pérez-Murano, P. Godignon, J. Camassel. Anisotropic growth of long isolated graphene ribbons on the C face of graphite-capped 6H-SiC. *Phys. Rev. B* **80**, 125410 (2009).
17. M. Valakh, V. Kiselov, V. Yukhymchuk, V. Dzhagan, A. Efanov, M. Tryus, A. Belyaev, D.R.T. Zahn. Free-standing graphene monolayers in carbon-based composite obtained from SiC: Raman diagnostics. *Phys. Status Solidi A* **211**, 1674 (2014).
18. K.R. Paton *et al.* Scalable production of large quantities of defect-free few-layer graphene by shear exfoliation in liquids. *Nature Mater.* **13**, 624 (2014).
19. A.C. Ferrari, J. Robertson. Interpretation of Raman spectra of disordered and amorphous carbon. *Phys. Rev. B* **61**, 14095 (2000).
20. L.M. Malard, M.A. Pimenta, G. Dresselhaus, M.S. Dresselhaus. Raman spectroscopy in graphene. *Phys. Rep.* **473**, 51 (2009).
21. F. Tuinstra, J.L. Koenig. Raman spectrum of graphite. *J. Chem. Phys.* **53**,1126 (1970).
22. S. Piscanec, M. Lazzeri, F. Mauri, A.C. Ferrari, J. Robertson. Kohn anomalies and electron-phonon interaction in graphite. *Phys. Rev. Lett.* **93**, 185503 (2004).
23. R. Beams, L.G. Cancado, L. Novotny. Raman characterization of defects and dopants in graphene. *J. Phys.: Condens. Matter* **27**, 083002 (2015).
24. E.H. Martins Ferreira, M.V.O. Moutinho, F. Stavale, M.M. Lucchese, R.B. Capaz, C.A. Achete, A. Jorio. Evolution of the Raman spectra from single-, few-, and many-layer graphene with increasing disorder. *Phys. Rev. B* **82**, 125429 (2010).
25. C. Casiraghi, S. Pisana, K.S. Novoselov, A.K. Geim, A.C. Ferrari. Raman fingerprint of charged impurities in graphene. *Appl. Phys. Lett.* **91**, 233108 (2007).
26. M.M. Lucchese, F. Stavale, E.H. Martins Ferreira, C. Vilani, M.V.O. Moutinho, R.B. Capaz, C.A. Achete, A. Jorio. Quantifying ion-induced defects and Raman relaxation length in graphene. *Carbon* **48**, 1592 (2010).
27. L.G. Cancado, A. Jorio, E. H. Martins Ferreira, F. Stavale, C.A. Achete, R.B. Capaz, M.V.O. Moutinho, A. Lombardo, T.S. Kulmala, A.C. Ferrari. Quantifying defects in graphene via Raman spectroscopy at different excitation energies. *Nano Lett.* **11**, 3190 (2011).
28. L.G. Cancado, K. Takai, T. Enoki, M. Endo, Y.A. Kim, H. Mizusaki *et al.* General equation for the determination of the crystallite size L_a of nanographite by Raman spectroscopy. *Appl. Phys. Lett.* **88**, 163106 (2006).
29. L.G. Cancado, M.A. Pimenta, B.R.A. Neves, M.S.S. Dantas, A. Jorio. Influence of the atomic structure on the Raman spectra of graphite edges. *Phys. Rev. Lett.* **93**, 247401 (2004).
30. C. Casiraghi, A. Hartschuh, H. Qian, S. Piscanec, C. Georgi, A. Fasoli, K.S. Novoselov, D.M. Basko, A.C. Ferrari. Raman spectroscopy of graphene edges. *Nano Lett.* **9**, 1433 (2009).
31. A. Eckmann, A. Felten, A. Mishchenko, L. Britnell, R. Krupke, K.S. Novoselov, C. Casiraghi. Probing the nature of defects in graphene by Raman spectroscopy. *Nano Lett.* **12**, 3925 (2012).
32. F. Banhart, J. Kotakoski, A.V. Krasheninnikov. Structural defects in graphene. *ACS Nano* **5**, 26(2011).
33. S.P. Lonkar, A.A. Abdala. Applications of graphene in catalysis. *Thermodyn. Catalys.* **5** (2), 1 (2014).

Received 10.09.16.
Translated from Ukrainian by O.I. Voitenko

В.О. Юхимчук, М.Я. Валах,
О.М. Грещук, Є.О. Гаврилюк, І.Б. Янчук,
А.В. Єфанов, Р.Н. Аріф, А.Г. Рожин, М.А. Скорик

ВЛАСТИВОСТІ ГРАФЕНОВИХ ФЛЕЙКІВ, ОТРИМАНИХ УЛЬТРАЗВУКОВОЮ ОБРОБКОЮ ГРАФІТУ

Р е з ю м е

В роботі продемонстрована можливість отримання графену та шарів на його основі за допомогою ультразвукової (УЗ) обробки піролітичного графіту в розчині N-метіл піролідону (NMP). Підтверджено, що ефективним методом діагностики процесу трансформації графіту в графен є рамановська спектроскопія. Варіюванням часу УЗ обробки піролітичного графіту в розчині NMP встановлені оптимальні режими отримання графенових флейків з різною кількістю шарів. Зокрема, показано, що УЗ обробка протягом 5 годин достатня для отримання колоїдного розчину графенових флейків, більшість з яких є одношаровими. Показано, що зі збільшенням часу УЗ обробки зростає інтенсивність раманівських смуг D та D', що свідчить про зростання кількості дефектів в графенових шарах. Оцінено середні відстані між дефектами при різних часах УЗ обробки. Проаналізовано вплив вакансійних та крайових дефектів на величину співвідношення $I_D/I_{D'}$ смуг та встановлено, що переважаючим типом дефектів в графенових флейках є вакансії.